MAGNETIC RESONANCE IN CHEMISTRY, VOL. 35, 629–636 (1997)

Side Chain Conformation of the Growth-Promoting Phytohormones Brassinolide and 24-Epibrassinolide†

Matthias Stoldt,[1] Andrea Porzel,[1] Günter Adam[1]* and Wolfgang Brandt[2]
[1] Institute of Plant Biochemistry, Weinberg 3, 06120 Halle/Saale, Germany
[2] Institute of Biochemistry, Martin-Luther-University Halle-Wittenberg, Kurt-Mothes-Strasse 3, 06099 Halle/Saale, Germany

Quantitative 2D NOE measurements and restrained molecular dynamics simulations (with explicit solvent) were carried out in order to determine preferential solution side chain conformations of the two most important native brassinosteroids, brassinolide and 24-epibrassinolide. The NOE assignment was assisted by 1D NOE difference spectroscopy and included prochiral assignment of the side chain methyl groups Me-26 and Me-27. 2D NOE intensities were converted into inter-proton distances using the 'complete relaxation matrix analysis' methodology. Restrained molecular dynamics simulations in a chloroform solvent box led to a well defined solution conformation in the case of brassinolide. The increased side chain flexibility in the case of 24-epibrassinolide is discussed, considering missing NOE correlations and vicinal proton coupling constants. © **1997 by John Wiley & Sons, Ltd.**

Magn. Reson. Chem. **35**, 629–636 (1997) No. of Figures: 4 No. of Tables: 3 No. of References: 21

Keywords: NMR; ^{1}H NMR; ^{13}C NMR; brassinosteroids; quantitative 2D NOE measurements; conformational analysis; molecular dynamics; solution conformation

Received 27 January 1997; revised 15 April 1997; accepted 22 April 1997

INTRODUCTION

Brassinosteroids are a new class of plant hormones showing high growth-promoting activity and other multiple effects on the growth and development of plants.[1] Since the discovery of brassinolide in rape pollen in 1979[2] as the first member, 37 native brassinosteroids have been characterized.[3] They all possess a 22*R*,23*R*-diol structural feature in the steroidal side chain which is essential for a high biological activity. Thus, compounds with 22*R*,23*R*-hydroxyls are much more active than synthetic analogues with 22*S*,23*S*-hydroxyls. On the other hand, in the native 22*R*,23*R*-configuration brassinosteroids members with a 24*S*-methyl or -ethyl group show a tenfold higher bioactivity than corresponding hormones with a 24*R*-alkyl function,[4] reflecting the significance also of the stereochemistry at this asymmetric centre. The two most important[5] phytohormones, brassinolide (**1**) and 24-epibrassinolide[6] (**2**) (Scheme 1), represent such an epimeric pair and were therefore selected for our conformational studies.

Whereas approaches using molecular modelling have been reported,[7,8] solution side chain conformation analysis of brassinosteroids based on NMR spectroscopy has not previously been carried out. Therefore, the aim of this work was to study whether brassinosteroids possess preferential solution conformations. Furthermore, we were interested in conformational differences of **1** and **2** and, should the occasion arise, in an explanation of the different bioactivities on the level of conformational behaviour. To do this, we mainly used quantitative 2D NOE measurements to collect conformation-restrictive information and molecular mechanics calculations for structure determination and refinement.

Concerning the present tremendous progress in molecular genetics of brassinosteroids,[9,10] such conformational studies are of special interest for future investigations on hormone–receptor interactions of this phytohormone group.

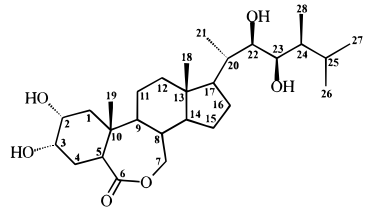

1

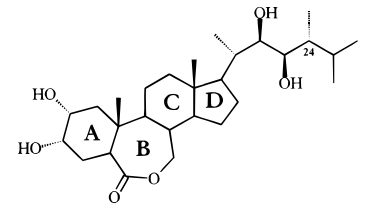

2

Scheme 1. Structures and numbering of brassinolide (**1**) and 24-epibrassinolide (**2**).

* *Correspondence to*: G. Adam.
† Dedicated to Professor Reiner Radeglia on the occasion of his 60th birthday.
Contract grant sponsor: Deutsche Forschungsgemeinschaft; *Contract grant number*: Po 581/1-1.

CCC 0749–1581/97/090629–08 $17.50

EXPERIMENTAL

A sample of **1** was purchased from Beak Technologies (Brampton, Canada). Compound **2** was prepared from ergosterol using a combination of the methods published by Thompson *et al.*[11] and Anastasia *et al.*[12]

NMR experiments

All NMR spectra were recorded at 301 K on a Varian UNITY-500 spectrometer operating at 499.835 and 125.70 MHz for ^{1}H and ^{13}C, respectively. For ^{1}H experiments, solutions of 0.5 mg of **1** and **2**, respectively, in 0.160 ml of $CDCl_3$ and a Nalorac 3 mm indirect detection probe were used; for ^{13}C experiments, a solution of 9 mg of **1** and 8 mg of **2** in 0.6 ml of $CDCl_3$–CD_3OD (95:5) (CD_3OD was used to give sufficient solubility) and a Varian 5 mm broadband probe were used. Chemical shifts were referenced to internal TMS ($\delta = 0$ ppm, ^{1}H) and $CDCl_3$ ($\delta = 77.0$ ppm, ^{13}C). Samples for NOE measurements were carefully degassed by five freeze–thaw cycles and then flame-sealed under an argon atmosphere.

All experiments were carried out using standard pulse sequences given by the manufacturers. All 2D spectra were recorded and processed in the phase-sensitive mode with quadrature detection in both dimensions.

1D ^{1}H NMR spectra. Size 32K, spectral width 5000 Hz, 80 scans, 0.8 s relaxation delay.

1D ^{13}C NMR spectra. Size 64K, spectral width 30 kHz, 4096 scans, 10 s relaxation delay, WALTZ-16 ^{1}H decoupling.

^{13}C T_1 measurements. Inversion–recovery pulse sequence, size 64K, spectral width 30 kHz, 14 recovery increments ranging from 0.001 to 18 s non-linear, 1600 scans per recovery increment, 10 s relaxation delay, WALTZ-16 ^{1}H decoupling.

1D TOCSY spectra with selective homodecoupling during acquisition. Size 128K, spectral width 2250 Hz, E-BURP-1 excitation pulse, two 2 ms trim pulses, 6.8 kHz spin lock field, 40 scans. The duration of spin lock period and power of homodecoupling were optimized to give the optimal signal amplitude and shape.

NOE difference spectra with or without selective homodecoupling during the acquisition period. Size 32K, spectral width 4000 Hz, 5 s relaxation delay, saturation time 3 s, alternating saturation of multiplet signals, 400–6000 scans, interleaved FID accumulation. FID was multiplied by a 0.5 Hz line-broadening exponential, difference spectra processing was performed in the frequency domain and the saturation and homodecoupling power were optimized to give the best selectivity.

COSY DQF spectra. Size in acquisition domain 1K, spectral width in F_1 and F_2 2250 Hz, 16 scans per each of 256 t_1 increments, 1.5 s relaxation delay.

NOESY spectra. Size in acquisition domain 2K and 4K, spectral width in F_1 and F_2 2250 Hz, 16, 32 or 64 scans per each of 256 or 512 t_1 increments, 100 ms–2.5 s mixing time, 1.5 or 2 s relaxation delay.

ROESY spectra. Size in acquisition domain 4K, spectral width in F_1 and F_2 2250 Hz, 2 kHz CW spin lock field, 32 scans per each of 512 t_1 increments, 400 and 600 ms mixing time, 1.5 s relaxation delay.

^{1}H–^{13}C HMQC spectra. Size in acquisition domain 1K, spectral width 10 kHz in F_1 (^{13}C), 2250 Hz in F_2 (^{1}H), 0.4 s delay after BIRD selection portion, polarization transfer delay to select $^1J_{CH} = 140$ Hz, 16 scans per each of 128 t_1 increments, GARP-^{13}C decoupling during acquisition, 1.8 s relaxation delay.

^{1}H–^{13}C HMBC spectra. Neither a BIRD selection nor ^{13}C decoupling was applied, the delay to select long-range correlations was set to 0.07 s, 80 scans per t_1 increment and other parameters identical with those of HMQC.

Determination of inter-proton distances

In order to relate NOESY cross peak intensities to inter-nuclear distances of the dipolar coupled proton pairs, NOESY spectra with a 400 ms mixing time were processed for both compounds with the NMR TRIAD program (SYBYL 6.2 software package, TRIPOS, St Louis, MO, USA). In both dimensions a 90° shifted squared sine-bell window function was applied and the F_1 dimension was zero-filled up to 2K data points. In the F_2 dimension a fourth-order polynomial baseline correction was used. Cross peaks which would be important for the determination of side chain conformations were integrated with manually determined baseline and peak boundaries. In cases where cross peaks appeared as resolved multiplets, they were integrated separately and added up.

We used the 'complete relaxation matrix analysis' program MARDIGRAS[13–15] as implemented in SYBYL 6.2 to obtain inter-proton distances. In a first step, all side chain NOE intensities, except the NOEs of Me-26 and Me-27 (not yet stereospecifically assigned), and additionally some well resolved NOEs of the steroidal skeleton (to give MARDIGRAS some experimental information on the sterically fixed part of the molecules) were used as program input. For the computation of distance ranges an estimate of experimental noise is necessary. This can be in the same units as the input NOE intensities, and so an averaged volume of 20 randomly selected noise peaks served as input. With the obtained distance range constraints the stereospecific assignment of the prochiral methyl groups Me-26 and Me-27 could be done in a first molecular modelling step (high-temperature restrained molecular dynamics, see below). Subsequently, a second MARDIGRAS distance computation with a new molecular input structure and all side chain NOE intensities was performed.

Molecular modelling

All molecular mechanics calculations were carried out on Silicon Graphics Power Indigo2 R8000, Indigo2 R4400 and Crimson R4000 computers using the

TRIPOS force field[16] of the molecular software package SYBYL 6.2.

To obtain the prochiral assignment for Me-26 and Me-27, high-temperature restrained molecular dynamics simulations were utilized. The first derived set of NMR upper and lower distances were added to the force field as pseudo-quadratic potentials with a force constant of 25 kcal mol^{-1} $Å^{-2}$. The simulation temperature and length were 1000 K and 100 ps, respectively; an NTV ensemble, an integration time step of 0.5 fs and a Boltzmann distribution of starting velocities were used. A non-bonded cut-off of 10 Å for van der Waals interactions was applied and non-bonded lists were updated every 5 fs. No electrostatic interactions were considered at this point. For both compounds, 100 conformations were extracted from the trajectory and energy minimized using the Powell method[17] until a gradient of 1×10^{-3} kcal mol^{-1} $Å^{-1}$ was achieved.

For further refinement, both brassinosteroids were surrounded with 645 chloroform solvent molecules (precomputed solvent box, 44.5 Å length in each dimension) and restrained energy minimization with the full set of distance range constraints (force constant 75 kcal mol^{-1} $Å^{-2}$) for 300 steepest descent and 5000 Powell steps was performed. Partial charge contributions were calculated using the method according to Gasteiger and coworkers[18,19] and electrostatic interactions were taken into account by using a constant dielectric function with $\varepsilon = 1$. Periodic boundary conditions were applied. Subsequently, the molecular ensembles were subjected to restrained molecular dynamics simulations at 300 and 500 K for 200 and 100 ps, respectively. The force field set-up and molecular dynamics parameters were identical with those of the energy minimization and the high-temperature simulations, respectively, except for the non-bonded reset which was set to 10 fs. From the trajectories six conformations of **1** and nine of **2** were selected manually, relating to different values of side chain dihedral angles. First, the whole molecular ensembles, including both the steroid and all solvent molecules, were energy minimized (1000 steps Powell method). Next, energy minimization to a gradient of less than 1×10^{-3} kcal mol^{-1} $Å^{-1}$ of only the steroid plus a 6 Å sphere of solvent molecules was performed.

In order to check whether the obtained conformations are stable without NMR-derived distance constraints concerning the TRIPOS force field, additional unrestrained 100 ps free molecular dynamics simulations at 300 K of selected starting conformations including the solvent field were carried out.

RESULTS AND DISCUSSION

Resonance assignment

^{1}H and ^{13}C resonance assignments of **1** and **2** have been carried out before.[20,21] In order to complete the ^{1}H assignment for **1**, to obtain accurate ^{1}H chemical shift values within the solution and measuring conditions used and to distinguish between the α and β protons of the steroidal skeleton, we re-assigned the ^{1}H and ^{13}C resonances of both compounds. We used a combination of 2D techniques (COSY DQF, HMQC, HMBC) as described in the previous paper.[20] The distinction of the diastereotopic protons (α and β) of the steroidal skeleton can easily be done by NOE difference spectroscopy with saturation of the two β-angular methyl groups Me-18 and Me-19 which give NOEs to all desired β protons. The ^{1}H and ^{13}C chemical shift values are given in Table 1.

NOE measurements and assignment

Before performing any NOE experiments with small- or medium-sized molecules, one should have an idea of the reorientation (molecular tumbling) behaviour of the molecule in solution because of the NOE's dependence on the correlation time τ_c. Since the NOE has a crossover point at $\omega\tau_c = 1.12$ and a fast variation around that point, it can be dangerous to interpret NOE data and convert them into three-dimensional structures if one has the case when $\omega\tau_c$ 1.12. To test this, we calculated the τ_c values of all methine group vectors from ^{13}C dipolar relaxation times for both brassinosteroids. Under extreme narrowing limit conditions, ^{13}C $T_{1,\mathrm{DD}}$ and τ_c relate in a simple manner:

$$\frac{1}{T_{1,\mathrm{DD}}(^{13}\mathrm{C})} = \left(\frac{\mu_0}{4\pi}\right)^2 \frac{\gamma_H{}^2 \gamma_{^{13}C}^2 \hbar^2 \tau_c}{r_{CH}^6}$$

where r_{CH} is the distance between the direct bonded carbon and hydrogen atoms. ^{13}C $T_{1,\mathrm{DD}}$ values were calculated from ^{13}C $T_{1,\mathrm{exp}}$ values (inversion–recovery

Table 1. ^{1}H and ^{13}C chemical shifts (ppm) of 1 and 2 in $CDCl_3$

	1		2	
Position	^{1}H	^{13}C	^{1}H	^{13}C
1	1.56/1.87[a]	41.5	1.55/1.87[a]	41.5
2	3.72	68.1	3.72	68.1
3	4.02	68.2	4.02	68.2
4	1.96/2.15[a]	31.0	1.95/2.14[a]	31.0
5	3.11	40.8	3.11	40.9
6	—	176.6	—	176.8
7	4.07	70.4	4.07	70.5
8	1.72	39.2	1.71	39.2
9	1.24	58.2	1.26	58.2
10	—	38.3	—	38.1
11	1.77/1.42[a]	22.2	1.77/1.40[a]	22.2
12	1.25/1.98[a]	39.6	1.22/1.98[a]	39.6
13	—	42.4	—	42.4
14	1.20	51.2	1.19	51.3
15	1.66/1.24[a]	24.7	1.68/1.26[a]	24.7
16	1.97/1.34[a]	27.5	2.01/1.33[a]	27.7
17	1.56	52.2	1.56	52.7
18	0.71	11.7	0.70	11.6
19	0.92	15.4	0.92	15.4
20	1.51	36.9	1.46	40.2
21	0.90	11.8	0.96	12.3
22	3.54	74.6	3.68	72.6
23	3.70	73.6	3.41	76.4
24	1.21	40.0	1.49	41.5
25	1.63	30.8	1.89	27.1
26^{proR}	0.96	20.8	0.87	17.3
27^{proS}	0.94	20.7	0.91	22.1
28	0.84	10.0	0.84	10.8

[a] α/β.

measurements) and ^{13}C signal intensities of 1D NMR spectra with and without $^{13}C\{^1H\}$ NOE:

$$\frac{1}{T_{1,\,DD}(^{13}C)} = \frac{1}{T_{1,\,exp}} \cdot \frac{2\gamma_{^{13}C}}{\gamma_{^1H}} \left(\frac{I_{\{^1H\}}}{I_0} - 1 \right)$$

The determined τ_c values appeared relatively uniform and a $\omega\tau_c$ value of 0.25 at a 500 MHz proton frequency results from an average τ_c of 0.08 ns (with respect to the measuring conditions).

NOESY spectra with different mixing times were recorded for both compounds (100–800 ms for **1** and 100 ms up to 2.5 s for **2**) to check the appearance of cross peaks. For mixing times of $\geqslant$150 ms a uniform set of NOE correlations could be found. This was the case up to 1.5 s. No further cross peaks appeared, and for mixing times >1.5 s a few disappeared. However, many of them were detectable even at a 2.5 s mixing time, indicating the rapid molecular tumbling. Most of the NOE correlations could be easily assigned and are trivial ones from the steroidal skeleton. Almost all side chain relevant cross peaks are located in two regions of the spectra—the methyl group region and the traces of H-22 and H-23 (see Fig. 1). To clear up some ambiguities in NOE assignment due to partial signal overlap, it was helpful to record 1D NOE difference spectra with saturation of either a methyl or an H-22 and H-23 resonance, benefitting from their high digital resolution. By comparing the exact chemical shifts and signal shapes of the ambiguous NOEs with unambiguous NOEs (e.g. from the two β-angular methyl groups Me-18 and Me-19 or from side chain methyl groups and their vicinal methine protons), it was possible to assign NOEs to H-12β or H-16α and H-12α or H-24 in the case of **1** and NOEs to H-12β or H-16α and H-20 or H-24 in the case of **2**. For the distinction of some NOEs to H-20 or H-24 (**2**) and the assignment of one NOE from Me-21 to either H-12β or H-24 (**1**), additional NOE difference spectra were recorded with selective decoupling of the Me-21 or Me-28 resonances during the acquisition time to collapse the multiplicity and signal shape of H-20 or H-24, respectively. For **1** the ambiguous NOE could be assigned to the pair Me-21–H-24. In the case of **2** it became obvious not only that H-22 and H-23 have NOEs to H-24 and H-20, respectively, but also that there are effects from their vicinal protons (H-20 and H-24, respectively), produced by either strong scalar coupling or real spatial closeness. Unfortunately, owing to the signal overlapping of H-20

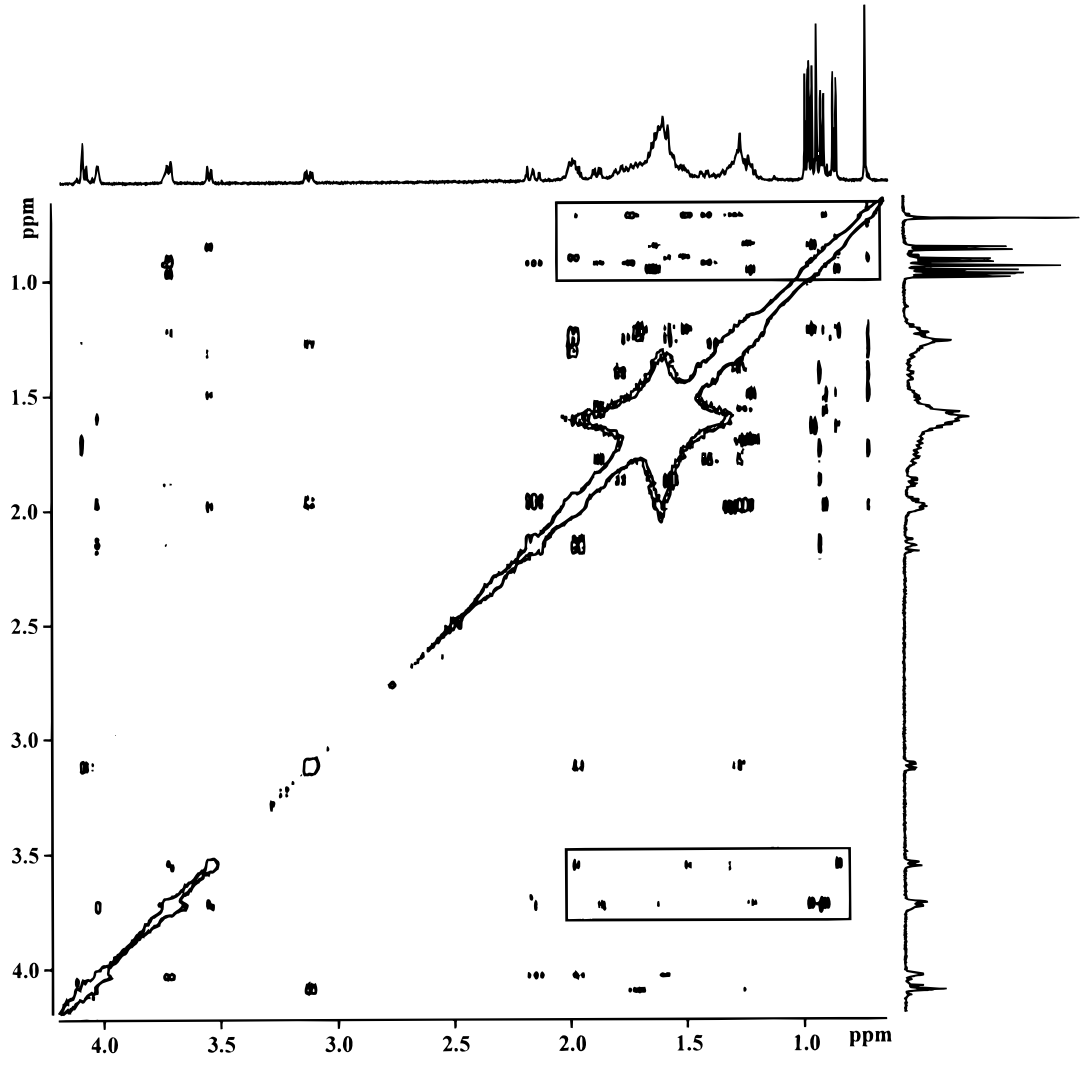

Figure 1. NOESY spectrum of **1** in $CDCl_3$. The mixing time was 400 ms. NOE cross peaks which are relevant for the side chain conformation are marked by rectangles.

and H-24 this made an exact integration of NOESY cross peaks impossible, and so we had to do without the quantitative information from these two NOE contacts.

An illustration of all side chain relevant NOE correlations is given in Table 2. The prochiral methyl groups Me-26 and Me-27 show different NOE correlations for both **1** and **2**. Furthermore, the NOE correlations are not equal if the two compounds are compared (see Fig. 2). In the case of **1** both methyl groups have an NOE contact to H-24 and one has a contact to H-23, whereas the other has a contact to Me-28. In the case of **2** there seems to be a simple spatial exchange of H-24 and Me-28 due to inversion of the C-24 stereo centre, because both methyl groups have a contact to Me-28, one to H-23 and the other to H-24. This suggests the existence of preferential side chain conformations in solution which should be different for both compounds.

Conformational analysis

To handle the conformation-restrictive NOE information in a computational molecular modelling procedure, one has to convert the NOE intensities into internuclear distances or, better, into distance ranges with respect to experimental and integration errors. There are different methods for converting these volume integrals into internuclear distances, including classification of the intensities into three different categories with corresponding distance ranges, 'isolated spin pair approximations' (ISPA) with a reference distance (including initial rate estimation from NOE built-up curves) and other approximations to determine the cross-relaxation (e.g. from ratios of cross and diagonal peak intensities). However, in order to analyse accurately NOESY intensities incorporating the effects of spin diffusion and network relaxation, the 'complete relaxation matrix analysis' method is used. Because of its special treatment of methyl groups, taking into account fast internal motion of the methyl protons due to methyl rotation, we used the MARDIGRAS[13–15] program as implemented in SYBYL 6.2. Together with a model structure, which was built with the SYBYL graphical interface, MARDIGRAS computes distance ranges of the correlated proton pairs by an iterative back-calculation of the rate matrix from the hybrid matrix of mixing coefficients (both experimental and theoretical ones which are proportional to the NOE intensities) and, subsequently, the distance matrix.[13] The choice of the 400 ms NOESY spectra was a compromise between poor signal-to-noise ratios at short mixing times, which would lead to large integration errors, and increased multiple spin effects at large mixing times. First, a set of distance range constraints without consideration of the Me-26 and Me-27 NOEs was obtained. High-temperature restrained 100 ps molecular dynamics simulations using SYBYL 6.2 and the TRIPOS force field at 1000 K with a small force constant for the penalty term of NOE distance violations (25 kcal mol^{-1} $Å^{-2}$) and, subsequently, energy minimization of 100 collected structures were carried out to investigate the spatial arrangement possibilities of Me-26 and Me-27. For **1**, only one conformational family resulted owing to the good fixation of H-24 and, therefore, of Me-28 in combination with the Me-28–H-25 NOE contact. This conformation fulfils the spatial closeness of H-24 to both methyl groups, Me-26 and Me-27, and of H-23 and Me-28 to one of each, as the NOE correlations demand. In the case of **2**, only one of two resulting conformational families is in accordance with the detected NOE contacts on the one hand and with non-appearing ones on the other. With the prochiral assignment of Me-26 and Me-27 (see Fig. 2), a second MARDIGRAS computation led to a complete set of distance ranges.

Table 2. 2D NOE correlations which are relevant for the side chain conformations of 1 and 2, with open circles indicating identical correlations and solid circles different correlations

	H-20	Me-21	H-22	H-23	H-24	Me-28	H-25	Me-26^{proS}	Me-27^{proS}	H-12β	H-16α	H-16β	H-17	Me-18
1														
H-20					●	●								○
Me-21				○	●					○			○	○
H-22					○	○					○	○	○	
H-23		○					●	○						
H-24	●	●	○					●	○					
Me-28	●		○				●		○			●[a]		
H-25				●		●								
Me-26^{proR}				○	●									
Me-27^{proS}					○	○								
2														
H-20				●										○
Me-21				○						○			○	○
H-22					○	○	●				○	○	○	
H-23	●	○				●		○						
H-24			○						○					
Me-28			○	●				●	○					
H-25			●											
Me-26^{proR}				○		●								
Me-27^{proS}					○	○								

[a] Only detected in an NOE difference spectrum.

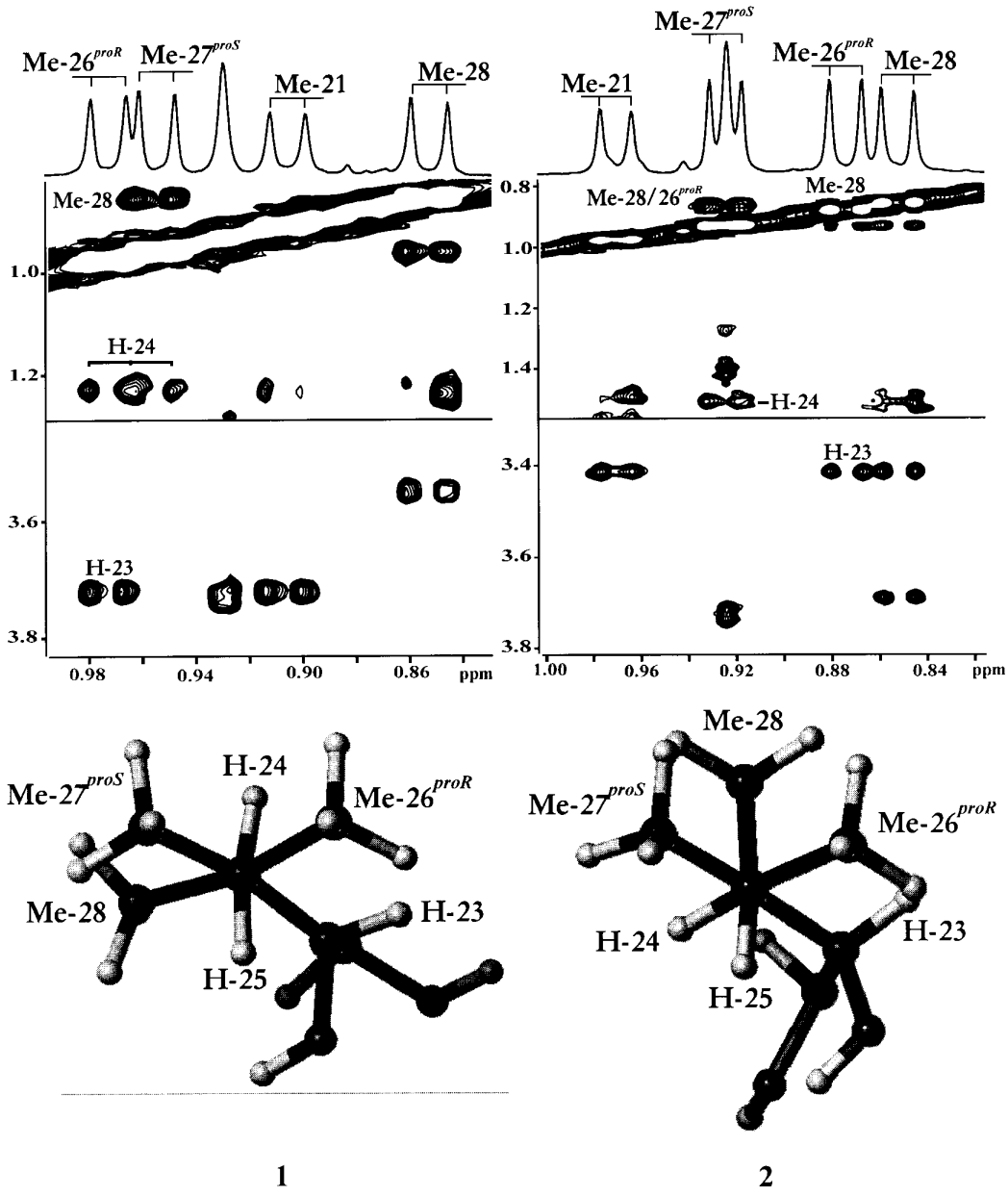

Figure 2. Prochiral assignment of Me-26^{proR} and Me-27^{proS}. Top: expansions of 400 ms NOESY spectra of **1** (left) and **2** (right) in $CDCl_3$ showing the differences in NOE correlations of Me-26^{proR} and Me-27^{proS}. Bottom: Newman projections of the C-24—C-25 bond.

Adding these constraints to the force field (force constant 75 kcal mol^{-1} Å^{-2}), further structure refinement using again molecular dynamics simulations was carried out. To take solvent effects into account, both brassinosteroids were soaked in solvent boxes of 645 $CHCl_3$ molecules. Simulations at 300 and 500 K with times of 200 and 100 ps, respectively, were analysed by monitoring the dihedral angles of the side chain.

In the case of compound **1**, all dihedral angles display a relatively constant time course with the exception of the dihedral angle describing the C-23—C-24 bond, which shows slightly more flexibility. Six snapshots were selected from the dynamics trajectory and energy minimized taking all solvent molecules into account, followed by an extensive energy minimization of the steroid molecule with a 6 Å sphere of the solvent. This led to structures satisfying all the NMR constraints and converged side chain conformation, again with the exception of the less populated structures with increased values of the fourth dihedral angle (H-23—C-23—C-24—H-24). The structures obtained are characterized by a *cis* arrangement of the 22*R*,23*R*-diol functionality and a kink at C-23 in the side chain conformation (see Fig. 3). In the case of compound **2**, a look at the time courses of the dihedral angles shows the increased fluctuation of third dihedral angle (H-22—C-22—C-23—H-23). Energy minimization of nine snap shots yielded structures for which the relative spatial position of the side chain varies starting at C-22. This is due to three possible values of the dihedral angle H-22—C-22—C-23—H-23. This leads to more or less extended conformations. However, the rear part itself is locally well defined (see Fig. 3). As all structures satisfy the distance range constraints, we had to discuss whether this flex-

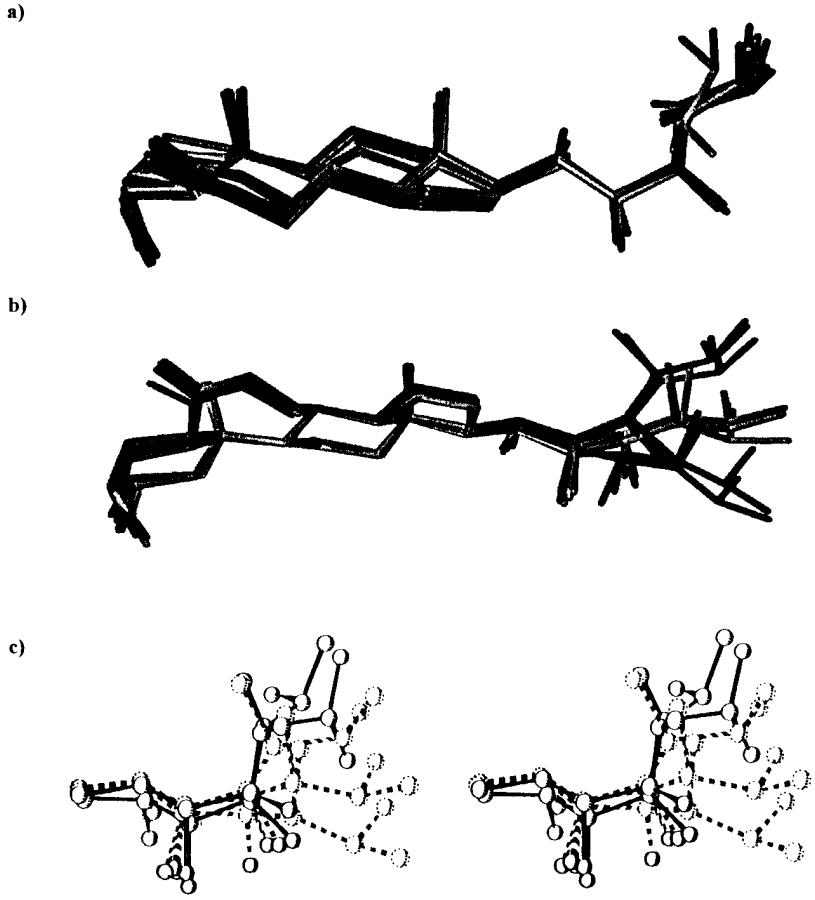

Figure 3. Representations of structures of **1** and **2** derived from restrained molecular dynamics simulations with explicit solvent. (a) Superposition of six structures of **1**. All heavy atoms were matched. (b) Superposition of nine structures of **2**. All heavy atoms of the steroid skeleton were matched. (c) Comparison of two structures of **1** and the three possible conformational families of **2**. The fit was made for the carbon atoms at positions 17, 20, 21 and 22.

ibility is a real feature of **2** or an effect of the lack of conformation-restrictive information (due to the signal overlap of H-20 and H-24) or of inaccuracy of the NOE intensity–distance data.

First, we found that in the case of the conformational family of **2** which exhibit large values of the H-22—C-22—C-23—H-23 dihedral angle, Me-28 has close spatial contacts to H-16β and H-20, which should give rise to NOEs. However, they could not be detected in either the NOESY spectra, the NOE difference spectra or the ROESY spectra (mixing times 400 and 600 ms) which were especially recorded for that purpose. From this we conclude that this conformational family is not the preferential one. Interestingly, for this conformation the rear side chain methyl groups as well as the hydroxyl group at position 23 adopt a very similar spatial arrangement to **1** (see Fig. 3). However, it is also clear that, if the flexibility of the rear part of the side chain is real, which would cause a fast and large fluctuation of the Me-28—H-16β and Me-28—H-20 distances, an NOE absolutely must not appear.

We also determined all vicinal proton coupling constants for the side chain of both compounds. In the case of H-22 and H-23, they could be taken from the 1D proton spectra. All other coupling constants were determined by 1D TOCSY experiments with selective excitation of side chain methyl protons or H-22 or H-23. To collapse the multiplicity of the signals to double doublets (H-20 and H-24) or doublets (H-25), the corresponding methyl protons were decoupled during the acquisition period. On a qualitative level the coupling constants support the NOE-derived conformations fairly well (see Table 3). In the case of **1**, the value of 1.7 Hz for the H-23–H-24 coupling constant seems to verify a corresponding dihedral angle of 60° more seriously than one of about 100°. To overcome the problem of multiple spatial side chain orientations in the molecular dynamics simulations of **2**, one can compare the H-22–H-23 coupling constants of **1** and **2**. Again, smaller dihedral angles seem to be favoured in the case of **2**. Unfortunately, a more precise conclusion cannot

Table 3. Experimental vicinal proton coupling constants (Hz) of the steroid side chain and dihedral angles (degrees) of refined conformations derived from restrained molecular dynamics simulations of 1 and 2

	1		**2**	
H/H	$^3J_{HH}$	Dihedral angle	$^3J_{HH}$	Dihedral angle
17/20	11.7	−177	11.2	−177
20/22	1.2	85	⩽1	56
22/23	8.4	−170	4.5	−85/−92/−133
23/24	1.7	60/98	6.3	160
24/25	8.1	−167	4.1	61

be drawn owing to the lack of suitable parameters for a Karplus relationship. Also, it is clear that fast interconversion of conformations could also produce an averaged value of 4.5 Hz for the H-22–H-23 coupling constant.

Additional free 100 ps dynamics calculations in solvent at 300 K for both brassinosteroids **1** and **2** without any constraints ensured that the structures obtained are stable and low-energy ones with respect to the force field used. The structures underwent no conformational changes. For **2** the same conformational behaviour concerning the fluctuation of the third side chain dihedral angle was observed.

CONCLUSION

The solution side chain conformations of the two native phytohormones brassinolide (**1**) and 24-epibrassinolide (**2**) were investigated by quantitative 2D NOE measurements and restrained molecular dynamics simulations with explicit solvent ($CHCl_3$). For **1**, one well defined solution structure was obtained, indicating that brassinosteroids are able to hold a preferential conformation. In the case of **2**, the H-22—C-22—C-23—H-23 dihedral angle appeared increasingly flexible from the molecular dynamics trajectory. This leads to different spatial orientations of the rear side chain, whereas this part itself is locally well defined. From NOE data and vicinal proton coupling constants it was not possible to decide whether this fluctuation is real or an artefact. Further investigations are necessary, e.g. extracting more conformation-restrictive information from heteronuclear coupling constants or alternative NOE measurements or proving the possible increased flexibility by detailed ^{13}C relaxation measurements. However, the more flexible conformational behaviour of **2** could explain its weaker bioactivity compared with **1**. The finding that one of the conformations of compound **2** found fits well that of compound **1** suggests the relevance of this conformation for putative hormone–receptor interactions.

Acknowledgements

The NMR microsample probe used was purchased with a grant from the Deutsche Akademie der Naturforscher Leopoldina. The work was supported by a grant from the Deutsche Forschungsgemeinschaft (Po 581/1-1). We thank Professor Dr M. Wiese, Institute of Pharmaceutical Chemistry, Martin-Luther-University Halle-Wittenberg, for providing calculation time on his SGI workstations.

REFERENCES

1. H. G. Cutler, T. Yokota and G. Adam (Eds), *Brassiosteroids—Chemistry, Bioactivity, Applications*, ASC Symposium Series, No. 474. American Chemical Society, Washington, DC (1991).
2. M. D. Grove, G. F. Spencer, W. K. Rohwedder, N. B. Mandava, J. F. Worley, J. D. Warthen, Jr, G. L. Steffens, J. L. Flippen-Anderson and J. C. Cook, Jr, *Nature* (*London*) **281**, 216 (1979).
3. G. Adam, A. Porzel, J. Schmidt, B. Schneider and B. Voigt, in *Studies in Natural Products Chemistry*, edited by Atta-ur-Rahman, Vol. 18, p. 495. Elsevier, Amsterdam (1996).
4. T. Yokota and K. Mori, in *Molecular Structure and Biological Activity of Steroids*, edited by M. Bohl and W. L. Duax, p. 318. CRC Press, Boca Raton, FL (1992).
5. H. G. Cutler, in *Natural and Engineered Pest Management Agents*, edited by P. A. Hedin, J. J. Menn and R. M. Hollingworth, ACS Symposium Series, No. 551, p. 85. American Chemical Society, Washington, DC (1994).
6. J. Schmidt, F. Böhme and G. Adam, *Z. Naturforsch., Teil C* **51**, 897 (1996).
7. T. C. McMorris, P. A. Patil, R. G. Chavez, M. E. Baker and S. D. Clouse, *Phytochemistry* **36**, 585 (1994).
8. C. Brosa, J. M. Capdevila and I. Zamora, *Tetrahedron* **52**, 2435 (1996).
9. A. Kauschmann, A. Jessop, C. Koncz, M. Szekeres, L. Willmitzer and T. Altmann, *Plant J.* **9**, 701 (1996).
10. S. D. Clouse, *Plant J.* **10**, 1 (1996).
11. M. J. Thompson, N. B. Mandava, J. L. Flippen-Anderson, J. F. Worley, S. R. Dutky, W. E. Robbins and W. Lusby, *J. Org. Chem.* **44**, 5002 (1979).
12. J. M. Anastasia, P. Allevi, P. Ciuffreda and A. Oleotti, *Steroids* **45**, 561 (1986).
13. B. A. Borgias and T. L. James, *J. Magn. Reson.* **87**, 475 (1990).
14. B. A. Borgias, M. Gochin, D. J. Kerwood and T. L. James, *Prog. Nucl. Magn. Reson. Spectrosc.* **22**, 83 (1990).
15. H. Liu, P. D. Thomas and T. L. James, *J. Magn. Reson.* **98**, 163 (1992).
16. M. Clark, R. D. Cramer, III and N. van Opdenbosch, *J. Comput. Chem.* **10**, 982 (1989).
17. M. J. D. Powell, *Math. Programming* **21**, 241 (1977).
18. J. Gasteiger and M. Marsili, *Tetrahedron* **36**, 3219 (1980).
19. J. Gasteiger and H. Saller, *Angew. Chem.* **97**, 699 (1980).
20. A. Porzel, V. Marquardt, G. Adam, G. Massiot and D. Zeigan, *Magn. Reson. Chem.* **30**, 651 (1992).
21. T. Ando, M. Aburatani, N. Koseki, S. Asakawa, T. Mouri and H. Abe, *Magn. Reson. Chem.* **31**, 94 (1993).

